On Mixed-mode Plane Stress Ductile Fracture

YIU-WING MAI and B. COTTERELL
Department of Mechanical Engineering, University of Sydney, Sydney, N.S.W. 2006, Australia

ABSTRACT

Mixed–mode ductile fractures in thin metal sheets are presented and analysed for two configurations: one is the in–plane mixed modes I and II failure and the other is the out–of–plane tearing modes III and I fracture. It is shown that truly mixed–modes I and II ductile failure can be obtained with the staggered deep edge notch tension specimen geometry which permits the mixed–mode J_c to be measured and to be partitioned into its component modes J_{Ic} and J_{IIc}. For metals with moderate necking and relatively large work hardening capacity J_c is approximately constant. However, for metals with intensive necking and low work hardening J_c varies with the staggered angle. The out–of–plane tearing modes III and I fractures can be obtained by using the trousers specimen geometry. It is difficult to separate the combined–mode J_c into its components J_{Ic} and J_{IIIc}.

KEYWORDS

Mixed–mode; tearing mode; ductile fracture.

INTRODUCTION

The design of structural components containing defects and flaws subjected to multiaxial loading requires a complete understanding of the mechanics and physics of mixed mode crack initiation and propagation. There are three basic modes of crack growth—crack opening mode (I), edge sliding mode (II) and out–of–plane tearing mode (III). Mixed mode crack growth concerns the combinations of any two modes of fracture, i.e. modes I/II, II/III and III/I. There are many practical examples of mixed mode crack growth. For example the delamination wear of metals and abrasive wear of viscoelastic materials like rubber [1,2] under sliding loads both involve modes I/II fractures; the crack initiation in the head of a rail due to a travelling load is a mixed mode II/III process [3]; and the tearing of ship plates by a rigid wedge representative of collision with a reef or iceberg is in modes III/I [4].

Much work has already been done in the past on mixed mode fractures of homogeneous isotropic brittle materials and a variety of criteria has been proposed for crack initiation [5–11] under mixed–mode I/II conditions. Though crack initiation may occur in mixed mode, once it is initiated, crack propagation reverts back to a single mode which is usually mode I for the cases of mixed modes I/II and I/III loading. Sometimes, reversion to either modes II or III can happen if a high enough superimposed pressure is sufficient to suppress mode I crack opening [12]. Although Broberg [12] has recently demonstrated that mixed mode II/III crack growth can take place in brittle solids with small scale crack tip yielding, it is generally impossible to produce truly mixed modes I/II and III/I crack propagation.

In ductile materials with large scale yielding under plane stress conditions, localised necks can form that in general are at an angle to the principal stresses so that mixed mode I/II crack propagation is permissible along the mid–line of the necking region. Previous attempts to investigate mixed mode I/II fracture in ductile solids are not very successful either because the fracture propagates in an essentially mode I direction [13] or the linear elastic fracture mechanics analysis employed is inappropriate [14]. The mixed mode III/I crack propagation can be achieved by the out–of–plane tearing of thin sheets that have undergone plastic bending and unbending. It must be remembered that true mixed mode ductile fractures can only occur in specimens that are completely yielded and where postyield fracture mechanics is required for the analysis of results. In this paper we are only concerned with ductile fractures in thin sheets of metals under mixed modes I/II and III/I.

CRITERIA FOR MIXED MODE DUCTILE FRACTURE

The most appropriate ductile fracture criterion is the critical J–integral (J_c) which is a measure of the specific essential work dissipated in the fracture process zone. For mixed mode I/II problems Ishikawa et al. [15] have shown that it is analytically possible to separate J_c into its component modes I (J_{Ic}) and II (J_{IIc}) so that $J_c = J_{Ic} + J_{IIc}$. Sakata et al. [16] conducted mixed mode I/II experiments on a 10 mm thick 2024–T351 aluminium alloy and showed that the initiation of stable crack growth followed the criterion:

$$J_{Ic} + J_{IIc} = J_c^*(\theta = 0^\circ) \tag{1}$$

where J_c^* ($\theta = 0^\circ$) is the critical J–integral for pure mode I loading, i.e. $\theta = 0^\circ$. According to this criterion for pure mode II loading, i.e. $\theta = 90^\circ$, $J_c^*(\theta = 90^\circ) = J_c^*(\theta = 0^\circ)$ so that both modes I and II have the same critical toughness. This conclusion is contradictory to the experimental results of Takamatsu and Ichikawa [17] who showed that for thin sheets of 2024–T3 aluminium alloy $\alpha J_c^*(\theta = 90^\circ) = J_c^*(\theta = 0^\circ)$, where $\alpha = 1.56$. This has led them to suggest that for ductile tear initiation the criterion should be modified to:

$$J_{Ic} + \alpha J_{IIc} = J_c^*(\theta = 0^\circ), \tag{2}$$

or alternatively to:

$$J_{Ic}/J_c^*(\theta = 0^\circ) + J_{IIc}/J_c^*(\theta = 90^\circ) = 1. \tag{3}$$

Experimental results on 1–mm thick sheets of slant center crack tension specimens do show that at crack initiation the net section stresses agree better with Equation (2). However, the differences between the stresses predicted from Equations (1) and (2) are no more than 10%. For practical purposes the fracture initiation criterion given by

Equation (1) may be well acceptable. In this specimen geometry the crack propagation is not mixed mode and its direction is almost perpendicular to the loading axis independent of the crack angle θ. True mixed mode fracture propagation is yet to be found. It should be noted at this point that the 2024–T3 has a relatively large work hardening exponent (n) as may be assessed from its yield (377 MPa) and tensile (507 MPa) strengths.

There is, strictly speaking, no theoretical basis for the fracture criteria of Equations (1) and (2). At best they are only phenomenological, if not empirical. In section 3.2 we report further ductile mixed mode fracture results for several other metallic materials for the critical evaluation of Equations (1) and (2).

As far as we are aware there is no ductile fracture criterion for mixed mode III/I failure. Indeed it would be difficult to separate the combined mode J_c into its component modes I and III, i.e. J_{Ic} and J_{IIIc}. In thin sheets containing a crack subjected to remote tensile loading it is reasonable to assume that J_c is largely determined by J_{Ic}. The contribution of J_{IIIc} is small and decreases as the sheet thickness is increased. On the other hand, thin sheets subjected to out–of–plane loading, such as in the trouser leg specimen geometry, J_c must be controlled by J_{IIIc} with a small contribution by J_{Ic} which may increase as the sheet thickness is increased. It might be possible to determine J_{IIIc} independently in guillotining experiments provided the clearance between the blade and the base plate is kept to a minimum. In practice, however, this would be rather difficult to achieve.

Because the out–of–plane tearing of thin metal sheets represents one of the basic forms of structural failure involving vehicle accidents in collisions, e.g. ship collisions resulting in the tearing of a thin plate by a sharp rigid wedge whereby energy absorption is in the form of tearing and plastic bending, there is considerable recent interest [18] in this failure mode and there is no need to separate mode I and mode III from the mixed mode J_c. In section 3.3 we present an energy balance analysis for the evaluation of J_c for this mixed mode III/I problem.

THE ESSENTIAL WORK OF FRACTURE APPROACH TO MIXED MODE PLANE STRESS DUCTILE FRACTURE

Concept of Specific Essential Fracture Work and Fracture Process Zone

In ductile fractures two zones can be identified at the crack tip. One is the inner zone where all fracture processes take place and this is conveniently called the fracture process zone (FPZ). The other is the outer plastic zone where irreversible plastic work is consumed and it acts as a filter allowing just enough energy to fracture the inner FPZ. This outer zone is dependent on loading configuration and specimen geometry. Only the work that is dissipated in the inner FPZ can be regarded as a material constant which is dependent on specimen thickness but independent of specimen geometry. This is called the specific essential work of fracture w_e by us which may be identified with J_c [19] and physically represents the work absorption in the FPZ. It is not possible a priori to determine the effects of mixed mode loading on w_e and J_c, although it is recognised that the FPZ size and the associated work absorption must be affected by the stresses acting on its boundaries. For example the fracture process zone width (d) is known to decrease from mode I to mode II fracture [19].

For thin sheets in mixed mode I/II the FPZ may be identified with the necking region at the crack tip (Fig. 1). If we assume that the equivalent stress–strain relationship for the material is given by the power law:

$$\bar{\sigma} = \sigma_o \bar{\epsilon}^n \tag{4}$$

where σ_o is a constant and n is the work hardening exponent, we can evaluate the J–integral around the boundary of the process zone to give the mixed mode J_c as:

$$J_c = d\int_o^{\bar{\epsilon}_n} \bar{\sigma}\, d\,\bar{\epsilon} + \int_{nd}^{\delta_{Ic}} \sigma\, d\,\Delta_I + \int_{ndcot\psi}^{\delta_{IIc}} \tau d\Delta_{II} \tag{5}$$

where σ, τ are stresses on the edge of the necked zone, Δ_I, Δ_{II} are the normal and tangential displacements of the necked zone which on entering the zone are nd and $ndcot\psi$ respectively, and $\bar{\epsilon}_n$ is the equivalent strain at the point of necking. ψ is the angle between the velocity discontinuity across the FPZ and the neck. Physically, the first term of the RHS of Equation (5) is the work to cause the formation of the neck, the second and third terms are associated with the work (tensile and shear components) to fracture the neck. J_c can be further separated into its mode I and mode II components as suggested in [15] such that:

$$J_{Ic} = \frac{\sin\psi\cos\theta}{\sin(\theta+\psi)} d\int_o^{\bar{\epsilon}_n} \bar{\sigma}\, d\,\bar{\epsilon} + \int_{nd}^{\delta_{Ic}} \sigma d\Delta_I \tag{6}$$

and

$$J_{IIc} = \frac{\cos\psi\sin\theta}{\sin(\theta+\psi)} d\int_o^{\bar{\epsilon}_n} \bar{\sigma}\, d\,\bar{\epsilon} + \int_{ndcot\psi}^{\delta_{IIc}} \tau d\Delta_{II}\,. \tag{7}$$

Pure mode I and mode II J_c values can be obtained by putting $\theta = 0°$ and $90°$ respectively into Equations (6) and (7). Since the critical opening displacements δ_{Ic} and δ_{IIc} are dependent on the ratio σ/τ it is impossible to compute these J_c integrals. Experimental evaluation becomes the only method of solution and this is described in section 3.2 using staggered deep edge notch tension specimens.

In the out–of–plane tearing mode III/I it is necessary to interpret the FPZ somewhat differently. The fracture process zone here involves a region of dimension s on either side of the torn edges which has undergone a plastic shearing strain γ_0 and a region of final tear which has been subjected to a mixed mode III/I failure (Fig. 2). The small necking in the fracture zone is due to mode I failure. The critical mixed mode J_c is therefore composed of two contributions: the plastic work in the shearing zone w_1 and the final tearing work w_2. Thus, we have

$$w_1 = 2s\int_o^{\gamma_o/\sqrt{3}} \bar{\sigma}\, d\,\bar{\epsilon} = \frac{2s\,\sigma_o\gamma_o^{n+1}}{(n+1)\,3^{(n+1)/2}}.$$

In unconstrained tearing the width of the shearing zone s is probably proportional to sheet thickness t. However, s can be varied in constrained tearing such as in guillotining and in the presence of grooves used to control the tear propagation direction [18]. For the tearing work we can estimate this to be:

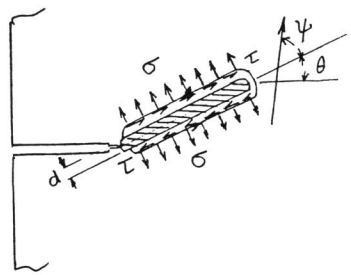

Fig. 1 – Evaluation of mixed mode J_c around boundary of FPZ

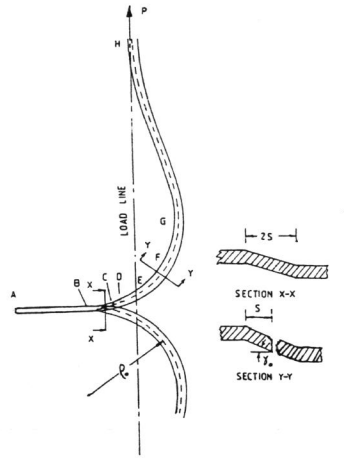

Fig. 2 – (a) Deformation configuration in I/II trousers specimen; (b) Section in FPZ undergoing plastic shearing; and (c) Final tear showing mixed mode III and I fractures.

$$w_2 = \frac{\sigma_o t\gamma_o^n}{2\,(3)^{(n+1)/2}} + t\int \bar{\sigma}\, d\,\bar{\epsilon} + \int \sigma\, d\,\Delta_I \tag{9}$$

with the first term for mode III and the second and third terms for mode I fractures. The mode I fracture work component is difficult to evaluate but for practical purposes it can be ignored. Thus,

$$J_c \doteq \frac{\sigma_o\,\gamma_o^n}{2\,(3)^{(n+1)/2}}\left[t + \frac{4s\,\gamma_o}{n+1}\right] \tag{10}$$

If $s \propto t$ then $J_c \propto t$ meaning that the specific essential fracture work increases linearly with sheet thickness in out–of–plane tearing of ductile solids. Experimental results on the tearing of a range of ductile sheet metals have been conducted by Rowe and Gurney [20] for thicknesses between 0.50 mm to 1.25 mm and these appear to support the prediction that J_c is proportional to t. However, recent work on constrained tearing of grooved trousers specimens of an aluminium alloy by Yu et al. [19] showed that $J_c \propto t^{0.61}$. The discrepancies observed between these results are not at all clear at this moment and further work is required to resolve this matter.

Mixed Mode I/II Fracture of Staggered Deep Edge Notch Tension Specimen

The staggered deep edge notch tension specimen geometry, Fig. 3, is the most suitable for obtaining true mixed mode fractures in ductile sheet metals. In these specimens localised necks form along the line joining the notches which develop into fractures when the tip of the notch reaches a critical opening displacement δ_c. For a given stagger

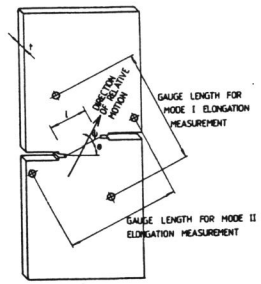

Fig. 3 – The staggered deep edge notch tension specimen.

angle θ there is a range of ligament lengths ℓ for which the cracks growing from the two notches would join up. The mode I and mode II works of fracture for a given ligament can be obtained from the area of the load–elongation curves recorded on an X–Y recorder. Because the work of fracture consists of two contributions – one from the essential work dissipated in the FPZ which is proportional to ℓ; and the other from the non–essential work consumed in the outer plastic zone which is proportional to ℓ^2 – we can plot the specific fracture work against ℓ to obtain a straight line relationship. J_{Ic} and J_{IIc} can be obtained by extrapolating the specific fracture work to zero ligament length. The mixed mode J_c is the sum of J_{Ic} and J_{IIc} for any given staggered angle.

Experimental results were obtained for four metals approximately 2 mm thick with the fractures propagated along the rolling direction. Their mechanical properties are given in Table 1. The low carbon steels, Lyten and TRLCS, have moderate necking and a

Table 1 – Mechanical Properties in Transverse to Rolling

Material	Lyten	TRLCS	5251	B1200–H14
0.2% proof stress (MPa)	360	320	132	112
UTS (MPa)	510	400	159	121
Elongation (%)	32	40	7	6
Strain hardening exponent (n)	0.25	0.10	0.05	0.05
Reduction in width (%)				
(a) Necked section	23	26	4	9
(b) Outside necked section	10	11	3	2
Reduction in thickness (%)				
(a) Necked section	28	24	57	75
(b) Outside necked section	6	10	3	2
Reduction in area (%)				
(a) Necked section	45	44	58	77
(b) Outside neck section	17	20	5	4

relatively large work hardening exponent. Conversely, the aluminium alloys, 5251 and B1200–H14, have intensive necking and a low work hardening exponent. Figures 4(a)–(d) show the mixed mode specific fracture work plotted against the ligament length for these four metals. Quite clearly, for the two low carbon steels, the mixed mode J_c is independent of the staggered angle, Figs. 4(a) and (b). These results confirm the mixed

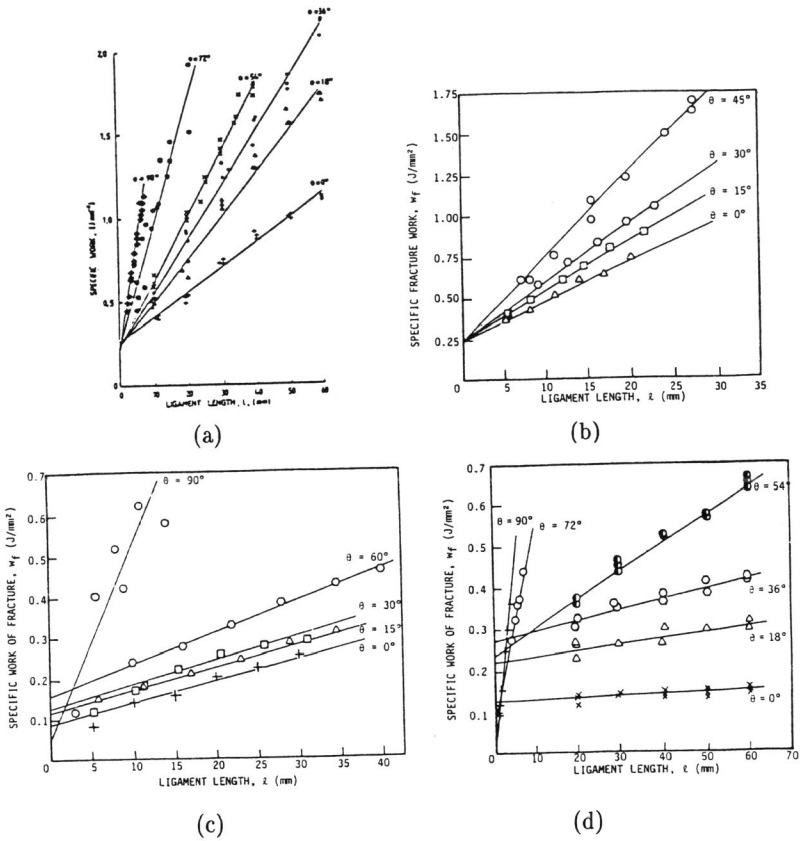

Fig. 4 Variation of mixed mode specific fracture work w_f with ligament length ℓ for (a) Lyten, (b) TRLCS, (c) 5251 and (d) B 1200–H14 staggered notched specimens.

mode fracture criterion of Equation (1), viz. $J_{Ic} + J_{IIc} = J_c^* \ (\theta = 0°)$. However, this fracture criterion does not hold for the aluminium alloys, Figs. 4(c) and (d), for J_c is now dependent on the staggered angle θ. Neither does the modified criterion suggested by Takamatsu and Ichikawa [18], i.e. Equations (2) or (3), as shown by the critical J–integral results in Fig. 5.

We can use Equations (5)–(7) to calculate J_c, J_{Ic} and J_{IIc} based on known values of d, δ_{Ic}, δ_{IIc} determined experimentally. This has been done in an earlier paper [21] and we do not wish to reproduce them here. Suffice to say, however, that the predicted mixed mode J_c is approximately independent of θ for the low carbon steels, but is dependent on θ for the aluminium alloys, in agreement with the experimental results given in Figs. 4(a)–(d). These theoretical results also show that for the steels, the work to form the neck is almost all the fracture work J_c; but for the aluminium alloys, this work component is only a small to moderate fraction of J_c. We, therefore, propose that the work hardening exponent (n) and the dimensional changes of the fractured neck in a tensile specimen largely determine if J_c is invariant with the stagger angle θ. If necking

is intensive and n is low, e.g. the aluminium alloys, J_c varies with θ. If necking is moderate and n is comparatively large, e.g. the low carbon steels, J_c is invariant with θ. This is only a hypothesis which seems to be reasonable and we do not claim to have any theoretical grounds for such a suggestion. The mixed mode fracture results mentioned in Section 2 by Sakata et al. [15] and Takamatsu and Ichikawa [16] on an aluminium alloy 2024–T3 and T–351 (with a relatively large n) seem to give some support to our hypothesis.

Mixed Mode III/I Fracture of Trousers Specimen

Out–of–plane tearing experiments were conducted on Lyten and aluminium 5251 using the two–leg trousers geometry shown in Fig. 2(a). The total work of fracture is the external work done by the applied tearing force P and the associated displacement due to a tear dx along the length of the leg. This work can be equated to the work of plastic shearing (w_1), tearing work (w_2) and the plastic bending and unbending work of the length dx(w_3). w_1 and w_2 are already given in Equations (8) and (9) and w_3 is obtained in [22] by:

$$w_3 = \frac{\sigma_o \, B t^{n+2}}{(n+1)(n+2)} \left[\frac{1}{\rho_o}\right]^{n+1} \tag{11}$$

so that

$$P/t = J_c/2 + \frac{\sigma_o B}{(n+1)(n+2)} \left[\frac{t}{\rho_o}\right]^{n+1} \tag{12}$$

where B is the width of the leg. Note that if n is small and approaching zero, then by substituting J_c with Equation (10) and assuming $s = \beta t$, we have

$$P = \frac{\sigma_o}{2}\left[\frac{1}{2\sqrt{3}} + \frac{2\beta\,\gamma_o}{\sqrt{3}} + \frac{B}{\rho_o}\right] t^2 = Kt^2. \tag{13}$$

Since for a given material K is a constant the tearing force P must be proportional to t^2 as shown by Rowe and Gurney [22].

The mixed mode J_c can be obtained by conducting a series of experiments on trousers specimens with varying leg width and plotting P/t against B. As shown in Fig. 6 a straight line relationship is expected and J_c is obtained by extrapolation to B = 0. Using Equation (8) we have calculated the plastic shearing (or burr formation) work to be 970 kJ/m² and 380 kJ/m² respectively for Lyten and 5251 based on experimental measurements of β, σ_o, n and γ_o [22]. These are substantial proportions of the mixed mode J_c. If we neglect the mode I contribution to w_2 in Equation (9) we can also estimate the mode III contribution, J_{IIIc}, which gives 310 kJ/m² and 100 kJ/m² for these two materials. These would represent the lowest possible values if tearing is purely mode III and plastic shearing can be completely suppressed. But in practical tearing situations, plastic shearing work and mode I fracture work are inseparable from the total fracture work. Hence, it is the mixed mode J_c determined from Equation (12) that is of the practical importance. Table 2 compares the critical J_c values in pure modes I, II and III for these two metals. It seems that mode II fracture work is the least and mode III fracture work the largest.

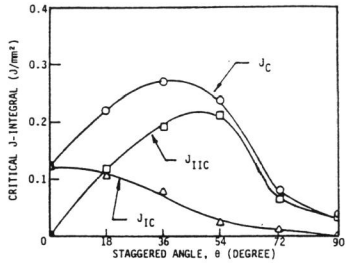

Fig. 5 Critical J–integral versus staggered angle for B1200–H14

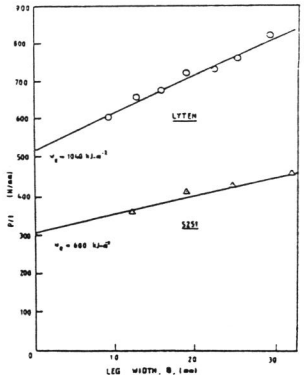

Fig. 6 Tearing force per unit thickness P/t plotted against leg width B for o Lyten and Δ 5251

Table 2 – Critical J–integral for Pure Modes I, II and III

Material		Lyten	5251
Mode I	J_c (kJ/m²)	250	85
Mode II	J_c (kJ/m²)	270	50
Mode III	J_c (kJ/m²)	1040 (370)*	600 (100)*

*Number in parenthesis is for pure mode III tearing without plastic shearing and mode I contribution.

CONCLUDING REMARKS

We have shown that it is possible to obtain true mixed mode I/II fractures in thin sheets of ductile metals using the staggered deep edge notch tension specimens. The critical mixed mode J_c and its component modes J_{Ic} and J_{IIc} can be obtained as a function of the stagger angle. There is no fracture criterion that is able to describe all the mixed mode fracture results although some success is achieved with the simple criterion: $J_{Ic} + J_{IIc} = J_c^*(\theta=0^0)$ for the low carbon steels. Mixed mode III/I fractures can be obtained in trousers specimens whose legs have undergone plastic bending and unbending. The plastic shearing work near the torn edges in unconstrained tearing is shown to be a substantial proportion of the total mixed mode J_c. There is a need to establish the dependence of J_c on sheet thickness since experimental results on both unconstrained and constrained tearing show disagreement with each other.

REFERENCES

1. Suh, N.P. (1981). *Fundamentals of Friction and Wear of Materials*, D.A. Rigney ed., ASTM, pp. 43–71.
2. Champ, D.H. (1974). Southern and A.G. Thomas, in *Advances in Polymer Friction Wear*, L.H. Lee ed., Plenum Press, pp. 133–144.
3. Chipperfield, C.G. (1981). Modelling rail head fatigue using fracture mechanics, *Proc. 34th Annual Conference of the Australian Institute of Megallurgists*, Surfers Paradise, Queensland, p. 63.
4. Vaughan, H. (1980). *J. Ship Res.*, 24, p. 96.
5. Erdogan, F. and G.C. Sih, (1963). *J. Basic Engg.*, 85, p. 519.
6. Williams, J.G. and P.D. Ewing (1976). *Int. J. Fract.*, 12, p. 85.
7. Cotterell, B. (1965). *Int. J. Fract.*, 1, p. 96.
8. Sih, G.C. (1974). *Int. J. Fract.*, 10, p. 305.
9. Ewing, P.D., J.L. Swedlow and J.G. Williams (1976). *Int. J. Fract.*, 12, p. 85.
10. Lee, D.J. and J.A. Donovan (1987). *Int. J. Fract.*, 34, p. 41.
11. Gent, A.N. and H.J. Kim (1978). *Rubber Chem. & Techn.*, 51, p. 35.
12. Broberg, K.B. (1987). *Engg. Fract. Mech.*, 28, p. 663.
13. Pook, L.P. (1971). *Engg. Fract. Mech.*, 3, p. 205.
14. Jones, D.L. and D.B. Chisholm (1975). *Engg. Fract. Mech.*, 7, p. 261.
15. Ishikawa, H., H. Kitigawa and H. Okamura (1979). In *Proc. ICM–3*, Vol. 3, K.J. Miller and R.F. Smith eds., Pergamon Press, pp. 447–455.
16. Sakata, M., S. Aoki, K. Kishimoto, M. Takizawa and H. Chikugo (1985/6). *Trans. Jpn. Soc. Mech. Eng.*, 51, p. 2129.
17. Takamatsu, T. and M. Ichikawa (1987). *J.S.M.E. Int. Journal*, 30, p. 265.
18. Yu, T.X., D.J. Zhang, Y. Zhang and Q. Zhou (1988). *Int. J. Mech. Sci.*, 30, p. 193.
19. Cotterell, B., E. Lee and Y–W. Mai (1982). *Int. J. Fract.*, 20, p. 243.
20. Rowe, P.W. and C. Gurney (1945). *Aero. Res. Comm., Repts and Memo. No. 2282, HMSO*, London, 6 pp.
21. Mai, Y.–W. and B. Cotterell (1983). In *Fracture Mechanics Technology Applied to Material Evaluation and Structure Design*, G.C. Sih et al. eds., Martinus Nijthoff, pp. 401–413.
22. Mai, Y–W. and B. Cotterell (1984). *Int. J. Fract.*, 24, p. 229.